Dynamic Distribution Factors

Abdullah Al-Digs, *Student Member, IEEE*, Sairaj V. Dhople, *Member, IEEE*,
and Yu Christine Chen, *Member, IEEE*

Abstract—This paper proposes an approach to obtain dynamic versions of static distribution factors, such as power-transfer, line-outage, and outage-transfer distribution factors. With the proposed *dynamic distribution factors* (DDFs), one can predict line flows over the post-contingency transient period with the same computational effort as obtaining static distribution factors. Our development centres on deriving closed-form expressions that approximate generator outputs through the post-contingency transient period with a reduced-order aggregate dynamical model to recover dynamic generator participation factors. The full suite of DDFs can then be derived by combining these dynamic generator participation factors with injection shift factors, i.e., static linear sensitivities of line active-power flows with respect to nodal active-power injections, computed at the pre-disturbance steady-state operating point. We illustrate the accuracy and computational benefits of the proposed DDFs via numerical case studies involving the New England test system.

Index Terms—Contingency analysis, distribution factors, injection shift factors, line-outage distribution factors, outage-transfer distribution factors, participation factors, power-transfer distribution factors, reduced-order models.
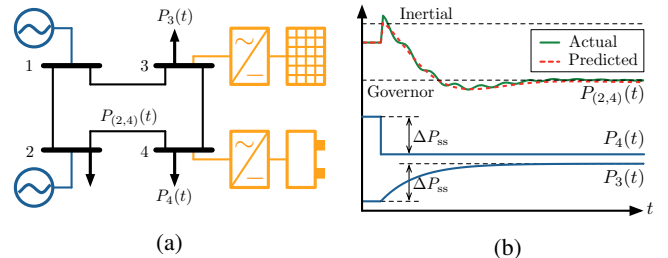
Fig. 1: Illustrating the dynamic PTDF. For the system in (a), consider time-varying injections at bus 3, $P_3(t)$, and at bus 4, $P_4(t)$, shown in the bottom pane of (b). This paper proposes a strategy with which one can predict line flows over the entire transient period while acknowledging load and synchronous-generator dynamics. As an example, the actual and predicted flows on line $(2,4)$, $P_{(2,4)}(t)$, are shown in the top pane of (b). Previous methods only acknowledge steady-state load changes (i.e., ΔP_{ss}) and yield estimates for a snapshot pertaining to inertial or governor response (dashed horizontal traces in top pane of (b)).

I. INTRODUCTION

THIS paper introduces the notion of and derives analytical closed-form expressions for dynamic distribution factors (DDFs): time-domain functions that approximate transients in post-contingency transmission-line flows synthesized with information collected from a pre-disturbance operating point and a reduced-order aggregate model for generator dynamics. The proposed DDFs acknowledge transients in injections (loads or renewable generation modelled as negative loads), and they improve upon conventional static distribution factors (DFs) that are applicable only at a single point in time. Furthermore, DDFs offer line-flow predictions with accuracy on par with running repeated time-domain simulations without the corresponding computational burden. In this work, without loss of generality, we derive dynamic counterparts of three commonly used static DFs [1]:

- Power-transfer distribution factor (PTDF), which approximates the post-disturbance steady-state sensitivity of the active-power flow in a line due to an active-power transfer between two buses.
- Line-outage distribution factor (LODF), which approximates the active-power flow change in a line due to the

outage of another line as a percentage of its pre-outage active-power flow.
- Outage-transfer distribution factor (OTDF), which approximates the sensitivity of the active-power flow in a line with respect to an active-power transfer between two buses after the outage of another line.

(See Fig. 1 for an illustration of how a dynamic PTDF allows one to capture transient line flows over a longer time horizon compared to its static counterpart.)

Static DFs are integral to a variety of power-system operations and control tasks such as contingency analysis, generation re-dispatch, and dynamic security assessment [1], and are therefore commonplace in commercial software packages such as Powerworld [2]. While static DFs provide fast contingency screening at the post-disturbance steady state, they only reveal point-in-time estimates and do not offer any insights on whether or not transmission-line flow limits would be violated during the transient period [1]. Performing repeated simulations with a detailed system dynamical model is the obvious alternative to gain more insight, but this is computationally expensive and therefore not suitable for online applications [3]. While we do not advocate or envision DDFs as a replacement for time-domain simulations, they may indeed prove useful in fast contingency screening. Furthermore, DDFs can replace their static counterparts in applications such as continuous-time economic dispatch (ED) for pricing of electricity and security-constrained ED. Approaches to approximate line-flow dynamics without excessive computational burden will be particularly relevant in operations and control tasks for next-generation power networks given that the retirement of fossil-fuel generation and integration of low-inertia electronics-interfaced generation will likely result in larger, faster, and
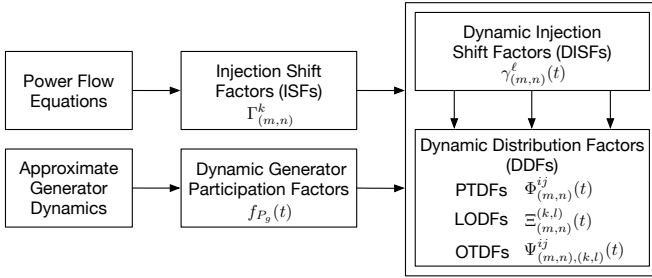
Fig. 2: Approach to obtain proposed DDFs. Conventional static DFs are obtained from generator participation factors that are valid for a single snapshot in time. In this work, we derive dynamic participation factors, $f_{P_g}(t)$, that extend the notion of static DFs through the post-contingency transient.

more frequent transient excursions away from steady-state operating points [4], [5].

We place subsequent discussions within the context of the flowchart in Fig. 2. There are two ingredients to obtain any (static or dynamic) DF: i) injection shift factors (ISFs) and ii) generator participation factors. The ISFs quantify the sensitivity of line flows with respect to variations in the active-power injection (generation or load) at a particular bus [1]. (In Fig. 2, the ISF capturing the sensitivity of change in injection at bus k on the flow in line (m,n) is denoted by $\Gamma^k_{(m,n)}$.) These are computed at the pre-disturbance steady-state operating point with a power-flow solution. In addition to the sensitivities, predicting line flows requires an estimate of how synchronous generators respond in restoring the system-wide generation-load balance. This is accomplished with so-called generator participation factors. Typically, participation factors are obtained by approximating generator outputs over time scales corresponding to inertial response, governor response, or economic dispatch [6]. Thus, they are valid for only a single snapshot in time. Unsurprisingly, DFs derived with such participation factors inherit their static nature [1], [7]–[9].

In this work, with a reduced-order model to describe system dynamics, we obtain dynamic generator participation factors which are valid over the entire post-disturbance transient period. (In Fig. 2, $f_{P_g}(t)$ denotes the dynamic participation factor for generator g.) Elementary algebraic operations on ISFs and dynamic generator participation factors then yield so-called dynamic injection shift factors (DISFs): time-domain functions that map a generation-load imbalance to the active-power flow on a line in the network. (In Fig. 2, the DISF capturing the sensitivity of change in injection at bus k on the flow in line (m,n) is denoted by $\gamma^k_{(m,n)}(t)$.) Finally, algebraic manipulations and combinations of DISFs yield a suite of DDFs such as PTDFs, LODFs, and OTDFs, all of which—it must be emphasized—are valid over the transient period capturing the evolution of post-disturbance dynamics to the new steady-state operating point.

Central to the procedure discussed above in obtaining DDFs are analytical closed-form expressions for dynamic generator participation factors $f_{P_g}(t)$. Essentially, these correspond to generator power outputs in response to net-load changes, but it is not possible to derive them from exact (e.g., two-axis) machine models. Instead, we leverage a second-order system-frequency-response model that maps load changes to

aggregate-frequency dynamics in closed form [10]–[13]. Then, using the aggregate frequency as a proxy for the individual-machine frequencies, we derive closed-form expressions that approximate individual generator power outputs. This enables us to obtain dynamic participation factors for any load-variation signals that are locally integrable. Without loss of generality, we focus on step and exponential-ramp changes for illustrative purposes. In fact, using the dynamic participation factors we derive for step changes in load, we recover static inertial-based DFs with $f_{P_g}(0)$ and governor-based DFs with $\lim_{t \to \infty} f_{P_g}(t)$. This is a notable contribution since static inertial- and governor-based DFs have been utilized with limited analytical justification in the literature [6].

This paper builds on our preliminary work in [14] and provides several extensions. First, while [14] focused exclusively on DISFs, here, we formulate and derive dynamic counterparts to well-known static DFs, including PTDFs, LODFs, and OTDFs. Also, while we previously only modelled step load-change disturbances, we extend the theoretical development to incorporate any general load-change signal that is locally integrable. Finally, we showcase the scalability of the proposed approach via numerical case studies involving the New England test system through an exhaustive simulation of 342 bilateral transactions. The proposed approach yields less than 1% average prediction error for 15732 simulated line flows (over the post-contingency transient period). The time-domain simulations required 9 hours to execute on a personal computer. On the other hand, the only computationally intensive part of our approach is the one-time task of computing the pre-disturbance power-flow solution to obtain the injection shift factors.

The remainder of this paper is organized as follows. In Section II, we define the proposed DISFs and discuss how DDFs are derived from these. Section III outlines the derivation of the dynamic generator participation factors. In Section IV, we focus on the derivation of the DDFs for the particular cases of step and exponential-ramp changes in load. We then demonstrate the utility of the proposed DDFs via numerical case studies involving the New England test system in Section V. Finally, concluding remarks and directions for future work are provided in Section VI.

II. Preliminaries and Definitions

In this section, we formally define the DISFs and introduce a suite of DDFs that can be obtained with them. (See Fig. 2.)

A. Dynamic Injection Shift Factors

Consider an AC network with nodes collected in the set $\mathcal{N}$, and let $\mathcal{G} \subset \mathcal{N}$ and $\mathcal{L} \subset \mathcal{N}$ denote the sets of generator and load buses, respectively. Transmission lines are collected in the set of edges $\mathcal{E} := \{(m,n)\} \subseteq \mathcal{N} \times \mathcal{N}$. We adopt the classical swing model augmented with a governor for generators, and loads are modelled as constant-power negative nodal injections. (A positive injection can be used to model, e.g., renewable generation.)

Denote the active-power load at bus $\ell \in \mathcal{L}$ by $P_\ell(t)$, and suppose that it changes as follows for time $t \geq 0$:

$$\Delta P_\ell(t) = f_{P_\ell}(t)\Delta P_{\ell,\text{ss}}, \qquad (1)$$

where $\Delta P_{\ell,\text{ss}}$ denotes the new steady-state value of the load, i.e., $\lim_{t\to\infty} \Delta P_\ell(t) = \Delta P_{\ell,\text{ss}}$, which implies that $\lim_{t\to\infty} f_{P_\ell}(t) = 1$. We assume that $f_{P_\ell}(t)$ is a continuously differentiable function that is known in analytical closed form. The formulation in (1) captures dynamics related to loads, which are dynamical systems in their own right [15], and renewable generation, which frequently exhibits ramp-like behaviour [16].

The total change in the active-power flow on line $(m,n) \in \mathcal{E}$ can be expressed as

$$\Delta P_{(m,n)}(t) = \gamma^\ell_{(m,n)}(t)\Delta P_{\ell,\text{ss}}, \qquad (2)$$

where $\gamma^\ell_{(m,n)}(t)$ denotes the DISF of line (m,n) with respect to bus ℓ, and it is given by

$$\gamma^\ell_{(m,n)}(t) := \sum_{g \in \mathcal{G}} \Gamma^g_{(m,n)} f_{P_g}(t) - \Gamma^\ell_{(m,n)} f_{P_\ell}(t). \qquad (3)$$

See Appendix A for a derivation of (3). Above, $\{f_{P_g}(t)\}_{g \in \mathcal{G}}$ are dynamic generator participation factors that capture how generators respond to the load change at bus ℓ. Particularly, with $\Delta P_g(t)$ denoting the change in the active-power output of generator g in response to the load change $\Delta P_\ell(t)$ given in (1), we define

$$f_{P_g}(t) := \frac{\Delta P_g(t)}{\Delta P_{\ell,\text{ss}}}. \qquad (4)$$

Furthermore, in (3), $\Gamma^k_{(m,n)}$ is the linear sensitivity of the active-power flow in line (m,n) with respect to the active-power injection at bus k computed at the pre-disturbance steady state.

While $\{\Gamma^k_{(m,n)}\}_{k \in \mathcal{N}, (m,n) \in \mathcal{E}}$ can be obtained from suitable manipulations of the power-flow equations around the pre-disturbance operating point, it is not straightforward to quantify the change in generator outputs, $\Delta P_g(t)$, in analytical closed form. Thus, it has been common practice to obtain $f_{P_g}(t)$ based on insights gleaned from economic dispatch, governor control, or synchronous-generator inertia characteristics [17]. For example, inertia-based participation factors are given by

$$f_{P_g} = \frac{M_g}{\sum_{k \in \mathcal{G}} M_k}, \qquad (5)$$

with M_g denoting the inertia constant for generator g; and governor-based participation factors are given by

$$f_{P_g} = \frac{R_g^{-1}}{\sum_{k \in \mathcal{G}} R_k^{-1}}, \qquad (6)$$

with R_g denoting the droop constant for generator g [6]. Note that these static participation factors are only valid at a particular snapshot in time. Furthermore, while governor-based participation factors can be recovered through a steady-state analysis of the generator dynamics, inertia-based participation factors have been proposed in the literature with limited analytical justification [6].

B. Common Dynamic Distribution Factors

With the DISFs defined above, we can obtain closed-form expressions for a suite of DDFs. We refer readers to [1], [18] for definitions of the corresponding static DFs.

1) Power-transfer Distribution Factor: Consider the scenario in which a time-varying injection at bus i,

$$P_i(t) = P_i(0) + \Delta P_i(t) = P_i(0) + f_{P_i}(t)\Delta P_{i,\text{ss}},$$

is matched by a time-varying withdrawal at bus j,

$$P_j(t) = P_j(0) + \Delta P_j(t) = P_j(0) + f_{P_j}(t)\Delta P_{j,\text{ss}},$$

with the steady-state constraint $\Delta P_{i,\text{ss}} = -\Delta P_{j,\text{ss}} = \Delta P_{\text{ss}}$. The dynamic PTDF approximates the post-disturbance sensitivity of the active-power flow in line (m,n) with respect to an active-power transfer of ΔP_{ss} from bus i to j. Particularly, the change in line (m,n) flow is approximated as

$$\Delta P_{(m,n)}(t) = \Phi^{ij}_{(m,n)}(t)\Delta P_{\text{ss}}, \qquad (7)$$

where the dynamic PTDF, denoted by $\Phi^{ij}_{(m,n)}(t)$, is given by

$$\Phi^{ij}_{(m,n)}(t) := \gamma^i_{(m,n)}(t) - \gamma^j_{(m,n)}(t). \qquad (8)$$

In the above,

$$\gamma^i_{(m,n)}(t) = \sum_{g \in \mathcal{G}} \Gamma^g_{(m,n)} f_{P_g}(t) - \Gamma^i_{(m,n)} f_{P_i}(t),$$

$$\gamma^j_{(m,n)}(t) = \sum_{g \in \mathcal{G}} \Gamma^g_{(m,n)} f_{P_g}(t) - \Gamma^j_{(m,n)} f_{P_j}(t),$$

are the DISFs of line (m,n) with respect to injections at buses i and j, respectively. Note that the dynamic participation factors in expressions for $\gamma^i_{(m,n)}(t)$ and $\gamma^j_{(m,n)}(t)$ are not the same, but we persist with this slight abuse of notation.

2) Line-outage Distribution Factor: Consider the scenario in which line (k,l) experiences an outage. The dynamic LODF approximates the active-power flow change in line (m,n) due to the outage of line (k,l) as a percentage of pre-outage active-power flow through line (k,l). Particularly, the change in line (m,n) flow can be approximated as

$$\Delta P_{(m,n)}(t) = \Xi^{(k,l)}_{(m,n)}(t)P_{(k,l)}(0), \qquad (9)$$

where the dynamic LODF, denoted by $\Xi^{(k,l)}_{(m,n)}(t)$, is given by

$$\Xi^{(k,l)}_{(m,n)}(t) := \frac{\Phi^{kl}_{(m,n)}(t)}{1 - \Phi^{kl}_{(k,l)}(t)} = \frac{\gamma^k_{(m,n)}(t) - \gamma^l_{(m,n)}(t)}{1 - \gamma^k_{(k,l)}(t) + \gamma^l_{(k,l)}(t)}. \quad (10)$$

3) Outage-transfer Distribution Factor: Consider the scenario in which after the outage of line (k,l), a time-varying injection at bus i of $P_i(t) = P_i(0) + \Delta P_i(t)$ is matched by a time-varying withdrawal at bus j of $P_j(t) = P_j(0) + \Delta P_j(t)$ where $\Delta P_{i,\text{ss}} = -\Delta P_{j,\text{ss}} = \Delta P_{\text{ss}}$. The dynamic OTDF approximates the post-disturbance sensitivity of the active-power flow in line (m,n) with respect to an active-power transfer from bus i to bus j after the outage of line (k,l). In particular, the flow on line (m,n) can be expressed as

$$\Delta P_{(m,n)}(t) = \Psi^{ij}_{(m,n),(k,l)}(t)\Delta P_{\text{ss}}, \qquad (11)$$

where the dynamic OTDF, $\Psi^{ij}_{(m,n),(k,l)}(t)$, is given by

$$\Psi^{ij}_{(m,n),(k,l)}(t) := \Phi^{ij}_{(m,n)}(t) + \Xi^{(k,l)}_{(m,n)}(t)\Phi^{ij}_{(k,l)}(t), \quad (12)$$

with $\Xi^{(k,l)}_{(m,n)}(t)$ denoting the dynamic LODF of line (m,n) with respect to an outage in line (k,l), and $\Phi^{ij}_{(k,l)}(t)$ denoting the dynamic PTDF of line (k,l) with respect to a power transfer from bus i to j.

C. Problem Statement

A suite of DDFs can be derived from the basic DISFs as defined in (3). Since DISFs are independent of the steady-state load change $\Delta P_{\ell,\mathrm{ss}}$, given a particular *type* of imbalance (e.g., step change, ramp change), our formulation yields line-flow estimates without any additional analytical or computational burden for different magnitudes of $\Delta P_{\ell,\mathrm{ss}}$. The enabling, and indeed novel, components in (3) are the dynamic participation factors for the generators, $\{f_{P_g}(t)\}_{g \in \mathcal{G}}$. Motivated by the single-snapshot participation factors in (5)–(6), we seek time-varying functions that delineate how generation-load mismatch is allocated among generators over the post-contingency transient period.

III. DYNAMIC GENERATOR PARTICIPATION FACTORS

This section introduces the synchronous-generator model and a corresponding second-order model with aggregate frequency and mechanical power inputs serving as states. With these models, we outline how generator power outputs can be approximated to yield dynamic generator participation factors.

A. Synchronous-generator Model

For each generator $g \in \mathcal{G}$, let $\omega_g(t)$, $P^{\mathrm{m}}_g(t)$, and $P_g(t)$ denote the electrical angular frequency, turbine mechanical power, and electrical-power output, respectively. Assume each generator initially operates at the steady-state equilibrium point with $\omega_g(0) = \omega_{\mathrm{s}} = 2\pi 60\,\mathrm{rad/s}$, the synchronous frequency. Defining $\Delta\omega_g := \omega_g - \omega_{\mathrm{s}}$, pertinent dynamics of generator $g \in \mathcal{G}$ can be described by [19]

$$M_g\Delta\dot{\omega}_g(t) = P^{\mathrm{m}}_g(t) - D_g\Delta\omega_g(t) - P_g(t), \quad (13)$$

$$\tau_g\dot{P}^{\mathrm{m}}_g(t) = P^{\mathrm{r}}_g - P^{\mathrm{m}}_g(t) - R^{-1}_g\Delta\omega_g(t), \quad (14)$$

where M_g and D_g denote, respectively, its inertia and damping constants, and τ_g, P^{r}_g, and R_g denote its governor time constant, reference power input, and droop constant, respectively. The generator dynamical model in (13)–(14) does not include dynamical models for the generator terminal voltage, automatic voltage regulators, or power-system stabilizers. Given the time-scales of interest, we find that the model in (13)–(14) is *sufficiently accurate* to capture the impact generator-frequency dynamics on line-flow transients. Furthermore, we do not consider nonlinearities, e.g., saturation limits. This is because we ultimately seek *closed-form* expressions for generator dynamic participation factors, a task that would be rendered intractable with the inclusion of nonlinearities.

B. Aggregate System Dynamical Model

Assume that the electrical distances between geographically different parts of the network are negligible, so that all generator frequencies follow the same transient behaviour [20], i.e., $\Delta\omega_g = \Delta\omega$ in (13)–(14), $\forall g \in \mathcal{G}$. Then, the dynamics of each generator g can be expressed as

$$M_g\Delta\dot{\omega}(t) = P^{\mathrm{m}}_g(t) - D_g\Delta\omega(t) - P_g(t), \quad (15)$$

$$\tau_g\dot{P}^{\mathrm{m}}_g(t) = P^{\mathrm{r}}_g - P^{\mathrm{m}}_g(t) - R^{-1}_g\Delta\omega(t). \quad (16)$$

If, further, the turbine time constants τ_g were equal for all generators, i.e., $\tau_g = \tau, \forall g \in \mathcal{G}$, then one could sum (15) and (16) over all $g \in \mathcal{G}$, define an aggregate mechanical power $P^{\mathrm{m}} = \sum_{g \in \mathcal{G}} P^{\mathrm{m}}_g$, and get the following reduced second-order system dynamical model:

$$M_{\mathrm{eff}}\Delta\dot{\omega}(t) = P^{\mathrm{m}}(t) - D_{\mathrm{eff}}\Delta\omega(t) - P_{\mathrm{load}}(t), \quad (17)$$

$$\tau\dot{P}^{\mathrm{m}}(t) = P^{\mathrm{r}} - P^{\mathrm{m}}(t) - R^{-1}_{\mathrm{eff}}\Delta\omega(t), \quad (18)$$

where, the *effective inertia constant*, M_{eff}, the *effective damping constant* D_{eff}, the *effective droop constant*, R^{-1}_{eff}, the aggregate reference power, P^{r}, and the total electrical load, P_{load}, are given by:

$$M_{\mathrm{eff}} := \sum_{g \in \mathcal{G}} M_g, \quad D_{\mathrm{eff}} := \sum_{g \in \mathcal{G}} D_g, \quad R^{-1}_{\mathrm{eff}} := \sum_{g \in \mathcal{G}} R^{-1}_g,$$

$$P^{\mathrm{r}} := \sum_{g \in \mathcal{G}} P^{\mathrm{r}}_g, \quad P_{\mathrm{load}} := \sum_{g \in \mathcal{G}} P_g. \quad (19)$$

In practice, while the turbine-governor time constants are (obviously) not all equal, they are quite similar in value for generators of the same type [21]. This has motivated several lines of work seeking suitable values of some common value of τ to yield the reduced-order model in (17)–(18). For instance, the average of τ_g's, for all $g \in \mathcal{G}$, is utilized in [10], [11]. More recently, the choice

$$\tau = \frac{\sum_{g \in \mathcal{G}}(R^{-2}_g + 1)}{\sum_{g \in \mathcal{G}}(R^{-2}_g + 1)\tau^{-1}_g} \quad (20)$$

is shown to minimize the Frobenius norm (an upper bound to the spectral norm) of the difference between pertinent matrices corresponding to the full- and reduced-order state-space models [12], [13].

C. Frequency-domain Analysis

The transfer function from load to aggregate frequency as derived from the state-space model in (17)–(18) is given by

$$\frac{\Delta\omega(s)}{P_{\mathrm{load}}(s)} = -\frac{k(s + \xi)}{s^2 + 2\zeta\omega_{\mathrm{n}}s + \omega^2_{\mathrm{n}}}, \quad (21)$$

where parameters k, ξ, ω_{n}, and ζ are, respectively,

$$k := M^{-1}_{\mathrm{eff}}, \qquad \xi := \tau^{-1}, \quad (22)$$

$$\omega_{\mathrm{n}} := \sqrt{\frac{R^{-1}_{\mathrm{eff}} + D_{\mathrm{eff}}}{\tau M_{\mathrm{eff}}}}, \quad \zeta := \frac{1}{2}\frac{M_{\mathrm{eff}} + \tau D_{\mathrm{eff}}}{\sqrt{\tau M_{\mathrm{eff}}(R^{-1}_{\mathrm{eff}} + D_{\mathrm{eff}})}}.$$

Suppose the load at bus $\ell \in \mathcal{L}$ changes by $\Delta P_\ell(t) = f_{P_\ell}(t)\Delta P_{\ell,\mathrm{ss}}$, as suggested in (1). The total load in the system can then be expressed as

$$
\begin{aligned}
P_{\mathrm{load}}(t) &= P_{\mathrm{load}}(0) + \Delta P_\ell(t) \\
&= P_{\mathrm{load}}(0) + f_{P_\ell}(t)\Delta P_{\ell,\mathrm{ss}}.
\end{aligned} \quad (23)
$$

With this generic load function, application of inverse Laplace transform of (21) yields the time-varying function $f_{\Delta\omega}(t)$ in analytical closed form so that one can express:

$$
\Delta\omega(t) = f_{\Delta\omega}(t)\Delta P_{\ell,\mathrm{ss}}. \quad (24)
$$

Differentiating (24), we get

$$
\Delta\dot{\omega}(t) = \frac{d}{dt}f_{\Delta\omega}(t)\Delta P_{\ell,\mathrm{ss}} =: f_{\Delta\dot{\omega}}(t)\Delta P_{\ell,\mathrm{ss}}, \quad (25)
$$

where, clearly, $f_{\Delta\dot{\omega}}(t)$ is also known in closed form.

D. Approximating Generator Outputs

We now shift focus to approximating the generator power outputs using (13)–(14) to derive the dynamic generator participation factors. First, approximating $\Delta\omega_g(t) \approx \Delta\omega(t)$ and further substituting $\Delta\omega(t) = f_{\Delta\omega}(t)\Delta P_{\ell,\mathrm{ss}}$ in (14), we get

$$
\tau_g \dot{P}_g^{\mathrm{m}}(t) = P_g^{\mathrm{r}} - P_g^{\mathrm{m}}(t) - R_g^{-1}f_{\Delta\omega}(t)\Delta P_{\ell,\mathrm{ss}}. \quad (26)
$$

Notice that this is a first-order differential equation in P_g^{m}, with a time-varying input $f_{\Delta\omega}(t)\Delta P_{\ell,\mathrm{ss}}$ that is known in analytical closed form. Therefore, we can obtain function $f_{P_g^{\mathrm{m}}}(t)$ in analytical closed form, such that

$$
P_g^{\mathrm{m}}(t) = P_g^{\mathrm{m}}(0) + f_{P_g^{\mathrm{m}}}(t)\Delta P_{\ell,\mathrm{ss}}. \quad (27)
$$

Next, rearranging terms in (13) while persisting with the approximation $\Delta\omega_g(t) \approx \Delta\omega(t)$, we get

$$
P_g(t) = P_g^{\mathrm{m}}(t) - D_g\Delta\omega(t) - M_g\Delta\dot{\omega}(t). \quad (28)
$$

Expressions for $\Delta\omega(t)$, $\Delta\dot{\omega}(t)$, and $P_g^{\mathrm{m}}(t)$ in (24), (25), and (27), respectively, can be substituted into (28) to yield:

$$
\begin{aligned}
P_g(t) = {}& P_g^{\mathrm{m}}(0) + f_{P_g^{\mathrm{m}}}(t)\Delta P_{\ell,\mathrm{ss}} \\
& - D_g f_{\Delta\omega}(t)\Delta P_{\ell,\mathrm{ss}} - M_g f_{\Delta\dot{\omega}}(t)\Delta P_{\ell,\mathrm{ss}}.
\end{aligned} \quad (29)
$$

Finally, recognizing that $P_g^{\mathrm{m}}(0) = P_g(0)$ at the initial pre-disturbance steady-state operating point, we can express (29) as $P_g(t) = P_g(0) + \Delta P_g(t)$, where

$$
\Delta P_g(t) = f_{P_g}(t)\Delta P_{\ell,\mathrm{ss}}, \quad (30)
$$

and the dynamic generator participation factor, $f_{P_g}(t)$, is

$$
f_{P_g}(t) := f_{P_g^{\mathrm{m}}}(t) - D_g f_{\Delta\omega}(t) - M_g f_{\Delta\dot{\omega}}(t). \quad (31)
$$

A closer inspection of (31) reveals that $f_{P_g^{\mathrm{m}}}(t)$ is derived using individual-governor time constants τ_g and droop constants R_g, while $f_{\Delta\omega}(t)$ and $f_{\Delta\dot{\omega}}(t)$ are related to the reduced-order model. Although the reduced-order model leverages an aggregated governor with a systematically determined time constant in (20), we preserve individual governor time constants and droop constants in approximating the generator outputs.

The dynamic participation factors, $f_{P_g}(t)$, can be computed for all generators $g \in \mathcal{G}$ and then substituted into (3) to yield closed-form expressions for DISFs. One can then obtain dynamic PTDFs, LODFs, and OTDFs with (8), (10), and (12), respectively. We derive dynamic generator participation factors for two typical instantiations of the time-domain load-change signal $\Delta P_\ell(t)$ next.

IV. DYNAMIC GENERATOR PARTICIPATION FACTORS FOR TYPICAL LOAD-CHANGE SIGNALS

In this section, we derive dynamic generator participation factors for step and ramp changes in the load. Indeed, with the approach outlined in Section III, one can consider countless different load changes. Our focus on step changes is motivated by uncovering inertial- and governor-based participation factors through an asymptotic analysis. Furthermore, step changes can be used to model generator outages, in which case dynamic participation factors for the remaining generators are derived for the post-contingency system. On the other hand, ramp changes are of interest as they can model fluctuations in renewable generation output [16]. More general time-domain functions that capture the outputs of solar-photovoltaic and wind-energy conversion systems could be similarly incorporated into the analytical framework.

A. Step Load Disturbance

Consider that the load at bus ℓ undergoes a step change at time $t = 0$ by $\Delta P_{\ell,\mathrm{ss}}$. From (23), for time $t > 0$, one can express the total system load, $P_{\mathrm{load}}(t)$, as

$$
P_{\mathrm{load}}(t) = P_{\mathrm{load}}(0) + \Delta P_\ell(t) = P_{\mathrm{load}}(0) + \Delta P_{\ell,\mathrm{ss}}. \quad (32)
$$

We substitute $P_{\mathrm{load}}(s) = \Delta P_{\ell,\mathrm{ss}}/s$ into (21), and follow the development in Sections III-C–III-D assuming the system is underdamped, i.e., $0 < \zeta < 1$, to get

$$
\begin{aligned}
f_{\Delta\omega}^{\mathrm{step}}(t) = {}& \frac{-1}{R_{\mathrm{eff}}^{-1} + D_{\mathrm{eff}}}\left(1 + \frac{\omega_{\mathrm{n}}}{\omega_{\mathrm{d}}}e^{-\zeta\omega_{\mathrm{n}}t}\cdot \right.\\
& \left. \left(\frac{\omega_{\mathrm{n}}}{\xi}\sin(\omega_{\mathrm{d}}t) - \sin(\omega_{\mathrm{d}}t + \varphi)\right)\right),
\end{aligned} \quad (33)
$$

$$
\begin{aligned}
f_{P_g^{\mathrm{m}}}^{\mathrm{step}}(t) = {}& \frac{R_g^{-1}}{R_{\mathrm{eff}}^{-1} + D_{\mathrm{eff}}}\left(1 - \frac{\tau_g^{-1}\omega_{\mathrm{n}}}{\omega_{\mathrm{d}}^2 + \theta_g^2}e^{-\zeta\omega_{\mathrm{n}}t}\cdot\right.\\
& \left(\frac{\omega_{\mathrm{n}}}{\xi}\cos(\omega_{\mathrm{d}}t) - \cos(\omega_{\mathrm{d}}t + \varphi)\right.\\
& \left.\left. + \frac{\theta_g}{\omega_{\mathrm{d}}}\sin(\omega_{\mathrm{d}}t + \varphi) - \frac{\theta_g}{\omega_{\mathrm{d}}}\frac{\omega_{\mathrm{n}}}{\xi}\sin(\omega_{\mathrm{d}}t)\right)\right),
\end{aligned} \quad (34)
$$

where the parameters ω_{d}, φ, and θ_g are given by

$$
\omega_{\mathrm{d}} := \omega_{\mathrm{n}}\sqrt{1 - \zeta^2}, \quad \varphi := \cos^{-1}(\zeta), \quad \theta_g := \tau_g^{-1} - \zeta\omega_{\mathrm{n}}. \quad (35)
$$

Furthermore, we take the time derivative of (33) to obtain a closed-form expression for $f_{\Delta\dot{\omega}}^{\mathrm{step}}(t)$. We substitute this resultant expression, along with $f_{\Delta\omega}^{\mathrm{step}}(t)$ and $f_{P_g^{\mathrm{m}}}^{\mathrm{step}}(t)$ in (33) and (34), respectively, into (31) to obtain dynamic generator participation factors, $f_{P_g}^{\mathrm{step}}(t)$, $\forall g \in \mathcal{G}$.

With the dynamic participation factors for step-load changes in place, we now derive the inertial- and governor-based participation factors in (5) and (6), respectively.

1) Revisiting Inertial-based Participation Factors: Inertial response occurs immediately after the load disturbance, so we recover the inertial-based generator participation factors by evaluating $f_{P_g}^{\text{step}}(0)$. Substituting for $f_{\Delta\omega}^{\text{step}}(0)$, $f_{\Delta\dot{\omega}}^{\text{step}}(0)$, and $f_{P_g^{\text{m}}}^{\text{step}}(0)$ in (31), we get:

$$f_{P_g}^{\text{step}}(0) = \frac{M_g}{M_{\text{eff}}} + \frac{R_g^{-1}}{R_{\text{eff}}^{-1} + D_{\text{eff}}} \cdot \frac{(\tau_g - \tau)R_{\text{eff}}^{-1}}{\tau_g R_{\text{eff}}^{-1} + (\frac{\tau}{\tau_g} - 1)M_{\text{eff}}}.$$

The inertial-based participation factors in (5) can be recovered from above under the assumption that all the governor time constants, τ_g, are equal.

2) Revisiting Governor-based Participation Factors: Governor-based participation factors are obtained at the post-disturbance steady state, so one can recover the governor-based generator participation factors by evaluating $\lim_{t\to\infty} f_{P_g}^{\text{step}}(t)$. Substituting for $\lim_{t\to\infty} f_{\Delta\omega}^{\text{step}}(t)$, $\lim_{t\to\infty} f_{\Delta\dot{\omega}}^{\text{step}}(t)$, and $\lim_{t\to\infty} f_{P_g^{\text{m}}}^{\text{step}}(t)$ in (31), we get:

$$\lim_{t\to\infty} f_{P_g}^{\text{step}}(t) = \frac{R_g^{-1} + D_g}{R_{\text{eff}}^{-1} + D_{\text{eff}}}.$$

If the damping constants are ignored, i.e., $D_g = 0$, $\forall g \in \mathcal{G}$, we recover the governor-based participation factors in (6).

B. Exponential-ramp Load Disturbance

Suppose that, starting at time $t = 0$, the load at bus ℓ follows an exponential ramp. Then, in accordance with (23), for $t > 0$, the total system load can be expressed as

$$\begin{aligned} P_{\text{load}}(t) &= P_{\text{load}}(0) + \Delta P_\ell(t) \\ &= P_{\text{load}}(0) + (1 - e^{-at})\Delta P_{\ell,\text{ss}}, \end{aligned} \quad (36)$$

where $a \geq 0$ is a constant. In the Laplace domain, the exponential-ramp load disturbance in (36) is given by

$$P_{\text{load}}(s) = \left(\frac{1}{s} - \frac{1}{s+a}\right)\Delta P_{\ell,\text{ss}}.$$

Substituting this Laplace transform into (21), taking the inverse Laplace transform of the resultant, and following the procedure described in Section III-C–III-D, we obtain:

$$f_{\Delta\omega}^{\text{ramp}}(t) = f_{\Delta\omega}^{\text{step}}(t) - \frac{1}{R_{\text{eff}}^{-1} + D_{\text{eff}}} \frac{\omega_{\text{n}}^2}{a^2 - 2\zeta\omega_{\text{n}}a + \omega_{\text{n}}^2} \quad (37)$$
$$\left(\upsilon e^{-at} - e^{-\zeta\omega_{\text{n}}t}\left(\upsilon\cos(\omega_{\text{d}}t) + (\rho+\eta)\sin(\omega_{\text{d}}t)\right)\right),$$

$$f_{P_g^{\text{m}}}^{\text{ramp}}(t) = f_{P_g^{\text{m}}}^{\text{step}}(t) + \frac{R_g^{-1}}{R_{\text{eff}}^{-1} + D_{\text{eff}}} \frac{\tau_g^{-1}\omega_{\text{n}}^2}{a^2 - 2\zeta\omega_{\text{n}}a + \omega_{\text{n}}^2}$$
$$\left(\frac{\upsilon}{\tau_g^{-1} - a}e^{-at} - \frac{\omega_{\text{d}}\upsilon + \theta_g(\rho+\eta)}{\omega_{\text{d}}^2 + \theta_g^2}e^{-\zeta\omega_{\text{n}}t}\sin(\omega_{\text{d}}t)\right.$$
$$\left. - \frac{\theta_g\upsilon - \omega_{\text{d}}(\rho+\eta)}{\omega_{\text{d}}^2 + \theta_g^2}e^{-\zeta\omega_{\text{n}}t}\cos(\omega_{\text{d}}t)\right), \quad (38)$$

where parameters υ, ρ, and η are given by

$$\upsilon := \frac{a}{\xi} - 1, \ \rho := \frac{a - \zeta\omega_{\text{n}}}{\omega_{\text{d}}}, \ \eta := \frac{\omega_{\text{n}}(\omega_{\text{n}} - a\zeta)}{\xi\omega_{\text{d}}}. \quad (39)$$

Unsurprisingly, since the load change in (36) represents the summation of a step change and an exponential-decay signal, the resulting time-domain solutions of $f_{\Delta\omega}^{\text{ramp}}(t)$ and $f_{P_g^{\text{m}}}^{\text{ramp}}(t)$

in (37) and (38), respectively, consist of the step response described in Section IV-A as well as dynamics arising from the exponential-decay input. Finally, similar to the procedure in Section IV-A, we substitute expressions for $f_{\Delta\omega}^{\text{ramp}}(t)$ in (37), its time derivative $f_{\Delta\dot{\omega}}^{\text{ramp}}(t)$, and $f_{P_g^{\text{m}}}^{\text{ramp}}(t)$ in (38) into (31) to arrive at dynamic generator participation factors for an exponential-ramp load change at bus $\ell \in \mathcal{L}$.

Remark 1 (Ramp Load Disturbance): In this remark, we note that the exponential-ramp load change in (36) can be used to approximate a ramp change in load. To see this, consider a ramp change in load at bus ℓ that initiates at time $t = 0$, so that the total system load can be expressed as

$$P_{\text{load}}(t) = \begin{cases} P_{\text{load}}(0) + \frac{\Delta P_{\ell,\text{ss}}}{t_{\text{r}}}t, & 0 \leq t < t_{\text{r}}, \\ P_{\text{load}}(0) + \Delta P_{\ell,\text{ss}}, & t \geq t_{\text{r}}, \end{cases} \quad (40)$$

where $t_{\text{r}} > 0$ is the ramp time. The Laplace transform of (40) is given by

$$\begin{aligned} P_{\text{load}}(s) &= \int_{t=0}^{t_{\text{r}}} \frac{\Delta P_{\ell,\text{ss}}}{t_{\text{r}}}te^{-st}dt + \int_{t=t_{\text{r}}}^{\infty} \Delta P_{\ell,\text{ss}}e^{-st}dt \\ &= \frac{\Delta P_{\ell,\text{ss}}}{s^2 t_{\text{r}}}(1 - e^{-st_{\text{r}}}). \end{aligned} \quad (41)$$

Similar to the derivation presented in Section IV-A, we can substitute the Laplace-domain load-disturbance signal in (41) into (21), take the inverse Laplace transform of the resultant, and apply suitable algebraic manipulations to obtain the corresponding dynamic generator participation factors. It turns out that this derivation is tedious and resulting closed-form expressions are lengthy and unwieldy. Thus, without loss of illustrative value and while limiting complexity, we approximate the ramp signal in (40) with the one in (36). Particularly, given the ramp time t_{r}, we can obtain an optimal value of the time constant a that minimizes the 2-norm of the error between signals described by (40) and (36) via the solution to the following unconstrained optimization problem:

$$\begin{aligned} \underset{a\in\mathbb{R}}{\text{minimize}} \quad &\int_{t=0}^{t_{\text{r}}} \left(\frac{\Delta P_{\ell,\text{ss}}}{t_{\text{r}}}t - \Delta P_{\ell,\text{ss}}\left(1 - e^{-at}\right)\right)^2 dt \\ &+ \int_{t=t_{\text{r}}}^{\infty} \left(\Delta P_{\ell,\text{ss}} - \Delta P_{\ell,\text{ss}}\left(1 - e^{-at}\right)\right)^2 dt. \end{aligned} \quad (42)$$

As detailed in Appendix B, the minimizer of (42) can be obtained by numerically solving

$$3at_{\text{r}} - 8\left(1 - e^{-at_{\text{r}}}\right) + 4at_{\text{r}}e^{-at_{\text{r}}} = 0, \quad (43)$$

given a particular ramp time t_{r}. Substitution of the optimal value of a, i.e., the solution of (43), into (36) yields an accurate approximation to the ramp-change signal in (40). We validate this through numerical results in Section V. $\blacksquare$

V. NUMERICAL SIMULATIONS

We illustrate concepts presented thus far with numerical case studies involving the New England (NE) 10-machine 39-bus test system. The topology of the network is shown in Fig. 3. Synchronous generators are connected to buses collected in $\mathcal{G} = \{30, \ldots, 39\}$, loads are connected to buses in $\mathcal{L} = \{1, 3, 4, 7, 8, 9, 12, 15, 16, 18, 20, 21, 23, \ldots, 29\}$, and the

system contains $|\mathcal{E}| = 46$ transmission lines. Although our analytical development is grounded in a simplified synchronous-generator model and leverages several approximations (e.g., common frequency deviation, no losses, etc.), we compare the line-flow predictions recovered from the proposed DDFs with time-domain simulations for a detailed, lossy, and nonlinear differential-algebraic model of the power network that includes dynamics from the two-axis synchronous generator, exciter, and governor. Simulations are performed using PSAT [22].

A. Illustrating Dynamic PTDFs, LODFs, and OTDFs

Here, we display a sample of results that can be obtained with the proposed DDFs for power-transfer and line-outage related contingencies. We simulate the following three scenarios: (a) the load at bus 8 increases via the ramp in (40) with $\Delta P_{8,\mathrm{ss}} = 0.5$ p.u. and $t_\mathrm{r} = 1$ s, balanced by a step load decrease at bus 1 in steady state, i.e., as in (32) with $\Delta P_{1,\mathrm{ss}} = -0.5$ p.u. (illustrated with ramp and step signals in red dashed lines in Fig. 3); (b) an outage on line $(16, 21)$ occurs at $t = 0$ s (encircled with a red dashed line in Fig. 3); and (c) scenarios (a) and (b) simultaneously.

Transient line flows from the time-domain simulation resulting from disturbance scenarios (a), (b), and (c) are plotted in Fig. 4 with solid traces. Dashed traces in Fig. 4 correspond to DDF-predicted transient line flows. To illustrate a sample of results, we plot flows for lines $(6, 7)$, $(23, 24)$, and $(3, 18)$ without loss of generality. Furthermore, the dash-dot traces represent transient line flows simulated with the exponential ramp-load increase at bus 8. By comparing the solid and dash-dot traces, we note that the dynamics arising from the exponential-ramp load-change signal indeed sufficiently approximate those from the exact-ramp load change. Closed-form expressions for dynamic PTDFs and OTDFs used to pre-

Fig. 4: Simulations for the NE system: actual and predicted line flows for a subset of lines due to (a) 0.5 p.u. power transfer between buses 8 and 1, (b) outage of line $(16, 21)$, and (c) scenarios in (a) and (b) triggered simultaneously.

dict transient line flows are derived with the less algebraically tedious exponential-ramp signal. Notice that the DDFs capture low-frequency dynamics in line flows in the transient period. Higher-order effects are attributable to voltage variations that our proposed approach does not capture.

B. Assessing Accuracy of the Proposed Approach

In this case study, we exhaustively implement the power-transfer scenario (a) in Section V-A for each pair of load buses in the NE system. Since there are 19 load buses and 46 lines, this case study involves $^{19}\mathrm{P}_2 = 342$ time-domain simulations for $342 \times 46 = 15732$ line flows. An illustration of a subset of simulation scenarios involved is depicted with step-ramp pairs (identical colours in solid lines alongside some load buses) in Fig. 3.

1) Acknowledging different governor time constants: We compare the actual and predicted line-flow dynamics and compute the average absolute error in each simulation over the entire simulation period of 3 s. These errors are visualized in the histogram in Fig. 5, where the x-axis represents the range of average line-flow errors and the y-axis displays the number of lines with errors in a particular range. The histogram coloured orange represents the case in which all governor time constants are set as $\tau_g = 0.7$ s, $g \in \mathcal{G}$, while the one coloured blue represents the case in which governor time constants are modified as follows: $\tau_{30} = 0.5$, $\tau_{31} = 0.6$, $\tau_{32} = 0.7$, $\tau_{33} = 0.4$, $\tau_{34} = 0.3$, $\tau_{35} = 0.7$, $\tau_{36} = 0.8$, $\tau_{37} = 0.7$, $\tau_{38} = 0.4$, $\tau_{39} = 0.5$ s. The average error over all lines and simulations is 0.0062 p.u. and the maximum error is 0.0747 p.u. for the case where all governor time constants are equal. By way of comparison, the average error over all lines and simulations is 0.0116 p.u. and the maximum error
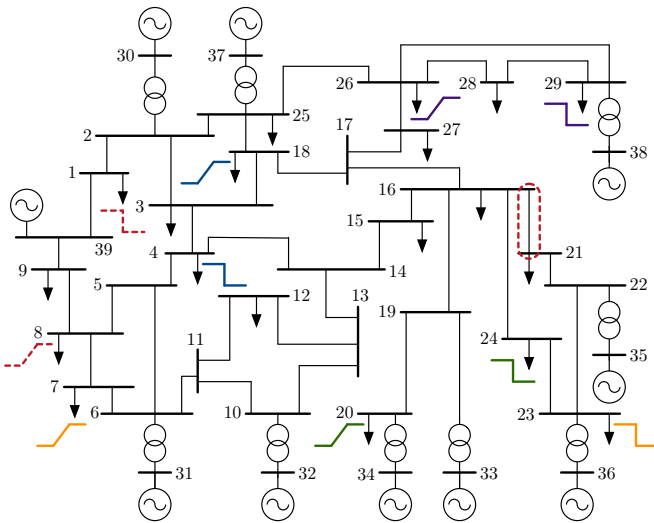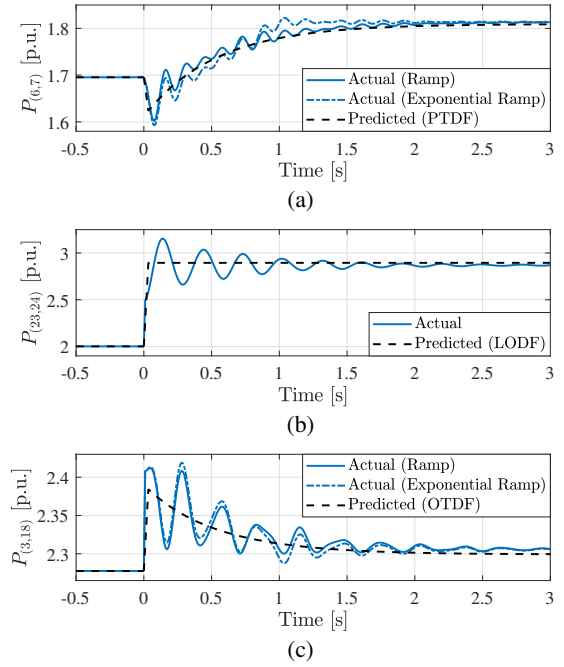

Fig. 3: Network topology for the New England system. Through simulations, we: i) Demonstrate that dynamic PTDFs, LODFs, and OTDFs yield transient line-flow predictions for contingencies involving an outage on line $(16, 21)$, ramp-load increase by 0.5 p.u. at bus 8, and step-load reduction by the same amount at bus 1. (These are illustrated in red dashed lines.); ii) Compute errors in line flows predicted with the proposed dynamic PTDFs for an exhaustive set of bilateral transactions between all load-bus pairs. (A sample of these transactions are illustrated with like-coloured ramps and steps in solid lines.)
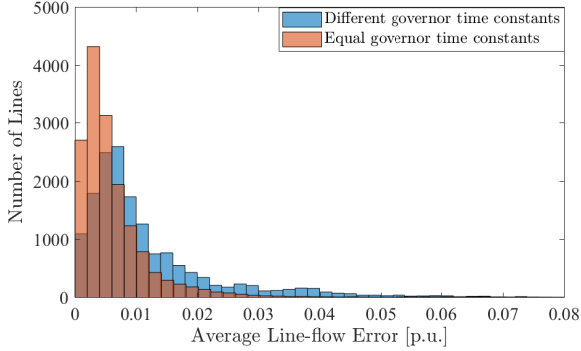
Fig. 5: Prediction errors for the NE system: average absolute error in line-flow predictions by dynamic PTDFs for an exhaustive set of step-ramp power transfers between all pairs of load buses. The histogram coloured orange represents the case in which all governor time constants are equal, while the one coloured blue represents one in which they are different.

TABLE I: New England system: comparison of number of post-contingency line-flow violations detected via time-domain simulations vs. the proposed closed-form DDF solution. Line limits that are 110%, 115%, 130%, and 150% of the pre-contingency line flows are examined.

Line Limit	110%	115%	130%	150%
Time-domain (PSAT)	983	603	277	113
Analytical (DDF)	950	603	277	112

is 0.078 p.u. with different governor time constants. In both cases, we use the choice in (20) for the time constant of the aggregate-governor dynamics. As expected, prediction errors increase in the case of different governor time constants. However, as we show next, the DDFs provide sufficiently accurate estimates of line flows to be used in fast contingency screening.

2) Fast contingency screening: While we do not advocate employing DDFs in place of time-domain simulations, they offer the ability to predict post-contingency line-flow violations with accuracy on par with that of time-domain simulations. To illustrate this, we list the number of violations for 110%, 115%, 130%, and 150% of the pre-contingency line flows that are uncovered using time-domain simulations versus DDFs in Table I. Note that governor time constants are modified so that they are different from each other, as listed in Section V-B1.

C. Comparing Computation Times

We record the computation required to perform a time-domain PSAT simulation of system dynamics in response to a step change in load and that needed to compute the corresponding closed-form DDF solution. The computation times required to conduct 3-, 5-, and 10-second simulations on a standard personal laptop are reported in Table II. We observe significant computational benefits compared to performing a detailed time-domain simulation, which suggests sizeable improvement for contingency screening in practice for a large-scale power system. In fact, the only computationally intensive step in predicting the line flows with the proposed approach relates to (the one-time task of) obtaining the pre-contingency power-flow solution to obtain the ISFs $\Gamma_{(m,n)}^k$, $\forall (m,n) \in \mathcal{E}$ and $\forall k \in \mathcal{L}$.

TABLE II: New England system: comparison of computing time required to estimate the post-contingency line flows for 3 s, 5 s, and 10 s due to a step change in load via time-domain simulations vs. the proposed closed-form DDF solution.

Duration of simulation [s]	3.00	5.00	10.0
Time-domain (PSAT) [s]	1.24	1.93	3.66
Analytical (DDF) [s]	0.0011	0.0013	0.0028

VI. CONCLUDING REMARKS AND DIRECTIONS FOR FUTURE WORK

We derived DDFs that are applicable throughout post-contingency transient periods by leveraging injection shift factors and dynamic generation participation factors. The proposed DDFs provide more insights compared to static distribution factors and present limited-to-no computational effort compared to running repeated time-domain simulations. The utility of the proposed expressions in accurately predicting post-contingency active-power line flows was demonstrated via numerical case studies involving the New England test system. A compelling avenue for future work is to explore how tasks pertaining to generation re-dispatch and dynamic security assessment can be reimagined with the proposed DDFs. Another avenue for future work is to extend the system-frequency model from the current setting with one coherent area to multiple coherent areas. Furthermore, closed-form expressions for participation factors of inverter-connected sources, such as solar photovoltaic and wind turbines, would be beneficial in the future. Finally, exhaustive simulations for different networks and contingencies may yield further insight on the accuracy and limitations of the proposed DDFs.

APPENDIX

A. Derivation of (3)

Collect nodal voltages, current injections, and complex-power injections in vectors $V \in \mathbb{C}^{|\mathcal{N}|}$, $I \in \mathbb{C}^{|\mathcal{N}|}$, and $S \in \mathbb{C}^{|\mathcal{N}|}$ respectively, and let $\theta \in \mathbb{T}^{|\mathcal{N}|}$ denote the vector of phase angles of the voltage phasors. It follows that $I = YV$, where Y is the network admittance matrix, and $S = \text{diag}(V)I^*$. Express the current flowing in line $(m,n) \in \mathcal{E}$ as

$$I_{(m,n)} = \left(y_{mn} e_{mn}^{\text{T}} + y_{mn}^{\text{sh}} e_m^{\text{T}} \right) V, \qquad (44)$$

where y_{mn} and y_{mn}^{sh} are, respectively, the series and shunt admittances of line (m,n). Substituting $V = Y^{-1}I$ above,

$$I_{(m,n)} = (\alpha_{(m,n)}^{\text{T}} + \text{j}\beta_{(m,n)}^{\text{T}})I, \qquad (45)$$

where $\alpha_{(m,n)}^{\text{T}} + \text{j}\beta_{(m,n)}^{\text{T}} := \left(y_{mn} e_{mn}^{\text{T}} + y_{mn}^{\text{sh}} e_m^{\text{T}} \right) Y^{-1} \in \mathbb{C}^{|\mathcal{N}|}$. Denote, by $S_{(m,n)} = P_{(m,n)} + \text{j}Q_{(m,n)}$, the complex power flowing across line (m,n), and by V_m the voltage at bus m. We can write

$$S_{(m,n)} = V_m I_{(m,n)}^*. \qquad (46)$$

Substituting (45) into (46) and making use of $I^* = \text{diag}(V)^{-1}S$, we obtain

$$S_{(m,n)} = V_m(\alpha_{(m,n)}^{\text{T}} - \text{j}\beta_{(m,n)}^{\text{T}})\text{diag}(V)^{-1}S. \qquad (47)$$

Taking the real part of (47), we get

$$P_{(m,n)} = \Gamma_{(m,n)}P + \varepsilon_{(m,n)}, \qquad (48)$$

where $\Gamma_{(m,n)} \in \mathbb{R}^{|\mathcal{N}|}$ and $\varepsilon_{(m,n)} \in \mathbb{R}$ are given by

$$\Gamma_{(m,n)} = |V_m| u_{(m,n)}^{\mathrm{T}}, \quad \varepsilon_{(m,n)} = -|V_m| v_{(m,n)}^{\mathrm{T}} Q. \quad (49)$$

Above, $u_{(m,n)}, v_{(m,n)} \in \mathbb{R}^{|\mathcal{N}|}$ are given by

$$u_{(m,n)} = \mathrm{diag}\left(\frac{\cos(\theta^m)}{|V|}\right)\alpha_{(m,n)} + \mathrm{diag}\left(\frac{\sin(\theta^m)}{|V|}\right)\beta_{(m,n)},$$

$$v_{(m,n)} = \mathrm{diag}\left(\frac{\sin(\theta^m)}{|V|}\right)\alpha_{(m,n)} - \mathrm{diag}\left(\frac{\cos(\theta^m)}{|V|}\right)\beta_{(m,n)},$$

where $|V| \in \mathbb{R}^{|\mathcal{N}|}$ is the vector of nodal-voltage magnitudes; $\cos(x)$ and $\sin(x)$ denote vectors with entries equal to the cosine and sine of respective entries of x; $\mathrm{diag}(x/y)$ denotes a diagonal matrix with diagonal entries composed of ratios of entries of vectors x and y; and $\theta^m := \theta_m \mathbb{1}_{|\mathcal{N}|} - \theta \in \mathbb{T}^{|\mathcal{N}|}$ with θ_m denoting the m-th entry of θ and $\mathbb{1}_{|\mathcal{N}|}$ denoting a length-$|\mathcal{N}|$ vector with all entries equal to 1. (Readers are referred to [23] for more details.) In practice, $\varepsilon_{(m,n)}$ is small for transmission-level lines where the active- and reactive-power decoupling assumptions are valid [24], and it can be neglected in (48).

The change in active-power flow in line (m,n), $\Delta P_{(m,n)}(t)$, due to variations in nodal active-power injections, denoted by $\Delta P_k(t)$, $k \in \mathcal{N}$, can be approximated from (48) as

$$\Delta P_{(m,n)}(t) = \sum_{k \in \mathcal{N}} \Gamma_{(m,n)}^k \Delta P_k(t), \quad (50)$$

where $\Gamma_{(m,n)}^k$ is the k-th entry of $\Gamma_{(m,n)}$ in (49). Now, consider the particular setting where the active-power demand at load bus $\ell \in \mathcal{L}$ changes by $\Delta P_\ell(t)$, and, in response, the changes in generator outputs are denoted by $\Delta P_g(t), g \in \mathcal{G}$. In this particular case, we get from (50) that the flow in line (m,n) can be approximated as

$$\Delta P_{(m,n)}(t) = \sum_{g \in \mathcal{G}} \Gamma_{(m,n)}^g \Delta P_g(t) - \Gamma_{(m,n)}^\ell \Delta P_\ell(t). \quad (51)$$

Substituting for $\Delta P_g(t)$ from (4) and for $\Delta P_\ell(t)$ from (1) in (51), we arrive at (3).

B. Derivation of Optimal Solution in (43)

We begin by expanding the objective function in (42) to get

$$\underset{a \in \mathbb{R}}{\text{minimize}} \; \Delta P_{\ell,\mathrm{ss}}^2 \left(\int_{t=0}^{t_\mathrm{r}} \frac{1}{t_\mathrm{r}^2} t^2 - \frac{2}{t_\mathrm{r}} t \left(1 - \mathrm{e}^{-at} \right) + 1 \right.$$
$$\left. - 2\mathrm{e}^{-at} + \mathrm{e}^{-2at} dt + \int_{t=t_\mathrm{r}}^{\infty} \mathrm{e}^{-2at} dt \right), \quad (52)$$

which can be simplified as

$$\underset{a \in \mathbb{R}}{\text{minimize}} \; \Delta P_{\ell,\mathrm{ss}}^2 \left(\frac{t_\mathrm{r}}{3} - \frac{3}{2a} + \frac{2}{a^2 t_\mathrm{r}} \left(1 - \mathrm{e}^{-a t_\mathrm{r}} \right) \right). \quad (53)$$

Then, applying the first-order necessary condition of optimality to (53) with respect to a, we get

$$0 = \frac{3}{2a^2} - \frac{4}{a^3 t_\mathrm{r}} (1 - \mathrm{e}^{-a t_\mathrm{r}}) + \frac{2}{a^2} \mathrm{e}^{-a t_\mathrm{r}}. \quad (54)$$

Multiplying both sides of (54) by $2a^3 t_\mathrm{r}$ yields (43).

REFERENCES

[1] A. J. Wood and B. F. Wollenberg, *Power generation, operation, and control*. John Wiley & Sons, 2012.

[2] T. J. Overbye and J. D. Weber, "Visualizing the electric grid," *IEEE Spectrum*, vol. 38, no. 2, pp. 52–58, Feb 2001.

[3] N. A. Samaan, L. Miller, J. Dagle, B. Vyakaranam, Y. Makarov, S. Wang, R. Diao, F. Tuffner, M. Vallem, and M. Pai, "Dynamic contingency analysis tool," *Pacific Northwest National Laboratory, Richland, Washington report-24843*, 2015.

[4] J. A. Taylor, S. V. Dhople, and D. S. Callaway, "Power systems without fuel," *Renewable and Sustainable Energy Reviews*, vol. 57, pp. 1322 – 1336, 2016.

[5] F. Milano, F. Dörfler, G. Hug, D. Hill, and G. Verbič, "Foundations and challenges of low-inertia systems," in *Power Systems Computation Conference*, Dublin, Ireland, Jun 2018, pp. 1–25.

[6] M. Lotfalian, R. Schlueter, D. Idizior, P. Rusche, S. Tedeschi, L. Shu, and A. Yazdankhah, "Inertial, governor, and AGC/economic dispatch load flow simulations of loss of generation contingencies," *IEEE Transactions on Power Apparatus and Systems*, vol. PAS-104, no. 11, pp. 3020–3028, Nov 1985.

[7] P. W. Sauer, "On the formulation of power distribution factors for linear load flow methods," *IEEE Transactions on Power Apparatus and Systems*, vol. PAS-100, pp. 764–779, Feb 1981.

[8] P. W. Sauer, K. E. Reinhard, and T. J. Overbye, "Extended factors for linear contingency analysis," in *Proc. of the Annual Hawaii International Conference on System Sciences*, 2001, pp. 697–703.

[9] T. Güler, G. Gross, and M. Liu, "Generalized line outage distribution factors," *IEEE Transactions on Power Systems*, vol. 22, no. 2, pp. 879–881, May 2007.

[10] P. M. Anderson and M. Mirheydar, "A low-order system frequency response model," *IEEE Transactions on Power Systems*, vol. 5, no. 3, pp. 720–729, Aug 1990.

[11] D. Apostolopoulou, P. W. Sauer, and A. D. Domínguez-García, "Balancing authority area model and its application to the design of adaptive AGC systems," *IEEE Transactions on Power Systems*, vol. 31, no. 5, pp. 3756–3764, Sep 2016.

[12] S. S. Guggilam, C. Zhao, E. Dall'Anese, Y. C. Chen, and S. V. Dhople, "Engineering inertial and primary-frequency response for distributed energy resources," in *Proc. of the IEEE Conference on Decision and Control*, 2017, pp. 5112–5118.

[13] S. S. Guggilam, C. Zhao, E. DallAnese, Y. C. Chen, and S. V. Dhople, "Optimizing DER participation in inertial and primary-frequency response," *IEEE Transactions on Power Systems*, vol. 33, no. 5, pp. 5194–5205, Sep 2018.

[14] A. Al-Digs, S. V. Dhople, and Y. C. Chen, "Time-varying injection shift factors to predict post-contingency dynamic line flows," in *Allerton Conference on Communication, Control, and Computing*, Oct 2017, pp. 302–306.

[15] D. Karlsson and D. J. Hill, "Modelling and identification of nonlinear dynamic loads in power systems," *IEEE Transactions on Power Systems*, vol. 9, no. 1, pp. 157–166, Feb 1994.

[16] R. Sevlian and R. Rajagopal, "Detection and statistics of wind power ramps," *IEEE Transactions on Power Systems*, vol. 28, no. 4, pp. 3610–3620, Nov 2013.

[17] Y. C. Chen, S. V. Dhople, A. D. Domínguez-García, and P. W. Sauer, "Generalized injection shift factors," *IEEE Transactions on Smart Grid*, vol. 8, no. 5, pp. 2071–2080, Sep 2017.

[18] J. Guo, Y. Fu, Z. Li, and M. Shahidehpour, "Direct calculation of line outage distribution factors," *IEEE Transactions on Power Systems*, vol. 24, no. 3, pp. 1633–1634, Aug 2009.

[19] P. W. Sauer and M. A. Pai, *Power System Dynamics and Stability*. Upper Saddle River, NJ: Prentice-Hall, Inc., 1998.

[20] M. D. Ilić and Q. Liu, *Toward Sensing, Communications and Control Architectures for Frequency Regulation in Systems with Highly Variable Resources*. New York, NY: Springer New York, 2012, pp. 3–33.

[21] R. Ramanujam, *Power System Dynamics: Analysis and Simulation*. PHI Learning Pvt. Ltd., 2009.

[22] F. Milano, "An open source power system analysis toolbox," *IEEE Transactions on Power Systems*, vol. 20, no. 3, pp. 1199–1206, Aug 2005.

[23] Y. C. Chen and S. V. Dhople, "Power divider," *IEEE Transactions on Power Systems*, vol. 31, no. 6, pp. 5135–5143, Nov 2016.

[24] J. Glover, M. Sarma, and T. Overbye, *Power System Analysis and Design*. Cengage Learning, 2008.

Abdullah Al-Digs (S'14) received the B.A.Sc. degree in electrical engineering (Power and Energy option) from The University of British Columbia, Vancouver, BC, Canada, in 2015, with distinction and was on the Dean's honour list. He is currently a Ph.D. candidate in the Department of Electrical and Computer Engineering at The University of British Columbia, where he is affiliated with the Power and Energy Systems research group. His research interests include power system analysis, operation, monitoring, and control.
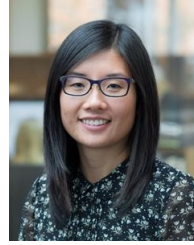
Yu Christine Chen (M'15) received the B.A.Sc. degree in engineering science from the University of Toronto, Toronto, ON, Canada, in 2009, and the M.S. and Ph.D. degrees in electrical engineering from the University of Illinois at Urbana-Champaign, Urbana, IL, USA, in 2011 and 2014, respectively. She is currently an Assistant Professor with the Department of Electrical and Computer Engineering, The University of British Columbia, Vancouver, BC, Canada, where she is affiliated with the Electric Power and Energy Systems Group. Her research interests include power system analysis, monitoring, and control.
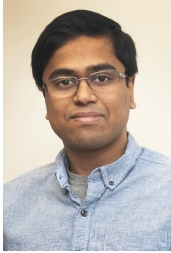
Sairaj V. Dhople (M'13) received the B.S., M.S., and Ph.D. degrees in electrical engineering from the University of Illinois at Urbana-Champaign, Urbana, IL, USA, in 2007, 2009, and 2012, respectively. He is currently an Associate Professor with the Department of Electrical and Computer Engineering, University of Minnesota, Minneapolis, MN, USA. His research interests include modeling, analysis, and control of power electronics and power systems with a focus on renewable integration. Dr. Dhople received the National Science Foundation CAREER Award in 2015 and the Outstanding Young Engineer Award from the IEEE Power and Energy Society in 2019. He is an Associate Editor for the IEEE TRANSACTIONS ON ENERGY CONVERSION and the IEEE TRANSACTIONS ON POWER SYSTEMS.